ScoreNet: A Neural Network-Based Post-Processing Model for Identifying Epileptic Seizure Onset and Offset in EEGs

Poomipat Boonyakitanont, Apiwat Lek-uthai, and Jitkomut Songsiri, *Member, IEEE*

***Abstract*— We design an algorithm to automatically detect epileptic seizure onsets and offsets from scalp electroencephalograms (EEGs). The proposed scheme consists of two sequential steps: detecting seizure episodes from long EEG recordings, and determining seizure onsets and offsets of the detected episodes. We introduce a neural network-based model called *ScoreNet* to carry out the second step by better predicting the seizure probability of pre-detected seizure epochs to determine seizure onsets and offsets. A cost function called *log-dice loss* with a similar meaning to the F_1 score is proposed to handle the natural data imbalance inherent in EEG signals signifying seizure events. ScoreNet is then verified on the CHB-MIT Scalp EEG database in combination with several classifiers including random forest, convolutional neural network (CNN), and logistic regression. As a result, ScoreNet improves seizure detection performance over lone epoch-based seizure classification methods; F_1 scores increase significantly from 16–37% to 53–70%, and false positive rates per hour decrease from 0.53–5.24 to 0.05–0.61. This method provides clinically acceptable latencies of detecting seizure onset and offset of less than 10 seconds. In addition, an *effective latency index* is proposed as a metric for detection latency whose scoring considers undetected events to provide better insight into onset and offset detection than conventional time-based metrics.**

***Index Terms*— Deep learning, EEG, EL-index, seizure onset and offset detection, ScoreNet.**

I. Introduction

AN EPILEPTIC seizure can be defined as a transient event of abnormal electrical activity in the brain [1]. Recently, epilepsy has affected approximately 65 million people around the world [2]. In clinical setting, neurologists can identify seizure characteristics through reviews of long scalp EEGs. However, the process of EEG visual examination is time-consuming, and prone to inconsistencies due to human errors brought by fatigue. To remove human errors from EEG-based seizure detection, we develop an automated epileptic seizure detection system that can label the time of seizure events in EEG signals. Several studies have developed methods to automatically detect epileptic seizures in EEG epochs [3]–[6]. Some studies focused on extracting single features relevant to EEG characteristics, e.g., amplitude [7]–[9], statistics [10], [11], entropy [12]–[14] and predictability [15]–[17]. Others have examined combinations of features to jointly distinguish between ictal patterns and normal activities [18]–[21]. In addition, recent studies have favored deep learning models to examine EEG signals because these models can implicitly extract latent features and classify seizure episodes themselves [22]–[25]. Some studies have focused on the designs and choices of deep learning architectures suitable for indicating seizures [26]–[29], whereas others have attempted to transform EEG segments into deep learning model inputs: e.g., an EEG plot image for a VGG16-based CNN model [30] and a three-dimensional EEG tensor for a temporal graph CNN model [31]. Still, despite the promising performances achieved by these epoch-based seizure detection methods, they have not been able to realistically infer seizure onsets and offsets. Both false positive and false negative outcomes are possible in epoch-based methods, despite a lack of abrupt ictal pattern changes. An issue of this is exemplified in Figure 1, where false negatives lead to mislabeling of seizure onsets/offsets that incorrectly interpret one seizure episode as multiple events. Conversely, many isolated false positives will cause frequent false alarms. Therefore, it is still clinically inappropriate to determine seizure onsets and offsets as the first and last epochs of seizures by existing epoch-based seizure classifiers.

While seizure detection has seen wide interest, only a few researchers have focused on seizure onset and offset detection. [32] proposed a method of detecting the endings of seizure episodes with a linear kernel support vector machine (linear SVM) using energies extracted from specific frequency bands of EEG epochs. However, this method failed to accurately determine seizure offsets when changes in seizure activity were gradual, and it needed a powerful seizure onset detector to satisfy its requirement of early seizure onset identification. [33] applied an artificial neural network (ANN) and linear discriminant analysis (LDA) with energy-based features calculated from stationary wavelet transform to determine seizures in EEG segments. Seizure onsets and offsets were then identified by the first and last indices of positive predictions during actual seizures. With discriminative features selected by a

Manuscript received May 17, 2021; revised October 15, 2021; accepted November 15, 2021. Date of publication November 19, 2021; date of current version December 8, 2021. This work was supported in part by the 100th Anniversary Chulalongkorn University Fund for Doctoral Scholarship, in part by the 90th Anniversary of Chulalongkorn University Fund (Ratchada-phiseksomphot Endowment Fund), and in part by the 2020 Chula Engineering Research Grant. *(Corresponding author: Jitkomut Songsiri.)*

The authors are with the Department of Electrical Engineering, Faculty of Engineering, Chulalongkorn University, Bangkok 10330, Thailand (e-mail: poomipatosk129@gmail.com; apiwat.l@chula.ac.th; jitkomut.s@chula.ac.th).

Digital Object Identifier 10.1109/TNSRE.2021.3129467

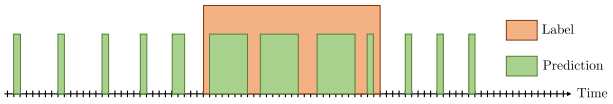

Fig. 1. Misinterpretation of seizure events from isolated false positives and false negatives.

feature selection method called Lambda of Wilks, LDA outperformed ANN in the seizure detection. Nevertheless, no evidence could be found from the mean onset and offset latencies to indicate that the proposed method determines seizure onsets/offsets accurately, thus it is possible that the seizure events were correctly detected, but only for part of the duration of the actual event. Recently, a CNN was proposed to spatially and temporally capture ictal patterns in EEG epochs [34]. This method included an additional post-processing procedure designed from clinical characteristics of seizures to reduce the occurrence of false positives and false negatives from prior classification. As a result, this method had a significantly improved F_1 score and drastically reduced FPR/h in almost all cases. However, the model parameters of this method were tediously manually selected for each patient which is a drawback that a self-learning scheme can address.

These issues encountered by previous epileptic seizure onset-offset detection methods were considered in the design of our automatic detection scheme which uses multi-channel scalp EEG signal inputs. Our detection system is divided into two sub-tasks: epoch-based classification, and onset-offset detection. The epoch-based classifier identifies seizures in small EEG segments independently and returns a predictive seizure probability as an output to the onset-offset detector. Several existing models including logistic regression, SVM, and decision tree can be applied in this first stage. Then, the second stage onset-offset detector receives as the input the preliminary results of epochs suspected of containing ongoing seizure occurrences, and estimates the starting and ending points of the detected events. This forms the first major contribution of our study: a novel model named *ScoreNet* that detects seizure onset-offsets by extending the detector structure in [34]. ScoreNet is a neural network-based model that automatically determines a group of seizure candidates from inputs, and then assigns a score to each candidate to determine the possibility that the candidate group should be regarded as a whole seizure activity. Such computations do not consider only a seizure epoch of interest, but also aggregate information from nearby epochs to take temporal changes of seizures into consideration. This feature makes ScoreNet unique from existing methods and improves the seizure detection performance from the first classification step. Moreover, since EEG seizure data are naturally highly imbalanced, the outcomes of existing detection methods tend to be biased towards a normal class. We address this issue by establishing a cost function in ScoreNet called *log-dice loss* based on a dice similarity coefficient.

Another issue in the abovementioned studies [33], [35] was that the mean latencies used for interpreting seizure onset-offsets were misleading; positive and negative latencies were defined as early and late predictions of seizure onset-offsets, respectively, and thus they could cancel each other out

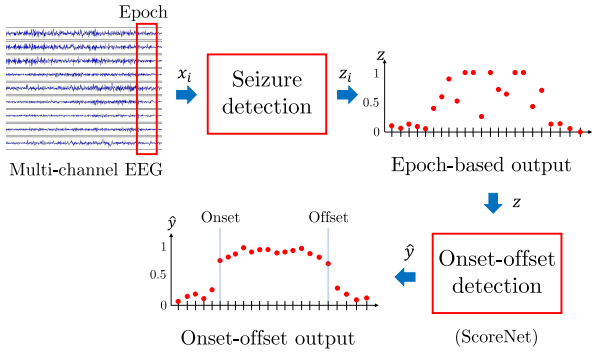

Fig. 2. A scheme for determining the seizure onset and offset in long EEG signal. In this work, the onset and offset detection using ScoreNet is mainly focused.

during the calculation of mean latencies. We address this issue by introducing the *effective latency index (EL-index)*, a novel time-delay metric that takes an undetected seizure onset-offset into consideration. Empirical results from this study will demonstrate that ScoreNet can dramatically reduce false positives and false negatives and precisely indicate seizure onsets and offsets from long EEG recordings. Additionally, it will be shown that using the log-dice loss helps overcome the class imbalance problem, and that the EL-index better represents the detection performance of a method than other conventional latency indices.

In summary, the contributions of this study are:

1) A neural network-based seizure onset and offset detector called *ScoreNet* and a loss function named *log-dice loss*.
2) A metric of onset-offset time delay termed the *effective latency index*.

This article is organized as follows: Section II presents the process of seizure onset-offset detection; Section II-B provides an in-depth explanation of ScoreNet; Section II-C provides the problem formulation including the proposed loss function; Section III describes the EL-index; Section IV outlines all the experiments conducted to verify ScoreNet; finally, Section V presents the seizure classification and seizure onset-offset determination results, accompanied by discussions and with graphical illustrations.

II. Methods

A. Detection Scheme

This research aspires to provide a method of detecting seizure episodes in long scalp EEGs and determining the onsets and offsets of the seizures. The detection process is divided into two sequential steps: epoch-based seizure classification, and seizure onset-offset detection, as shown in Figure 2. Firstly, long multi-channel EEGs are segmented into small multi-channel EEG epochs to be used in seizure classification. A classifier receives raw data or a feature vector from epoch i as the input x_i and produces a seizure probability z_i. An onset-offset detector then converts a collection of the prediction sequence $z = (z_1, z_2, \ldots, z_N)$ into the modified sequence of seizure probabilities $\hat{y} = (\hat{y}_1, \hat{y}_2, \ldots, \hat{y}_N)$ as a screened prediction of seizures. Finally, the onset and offset are indicated by the first and last indices of each predicted seizure that $\hat{y}_i \geq 0.5$, respectively. Onset-offset detection is

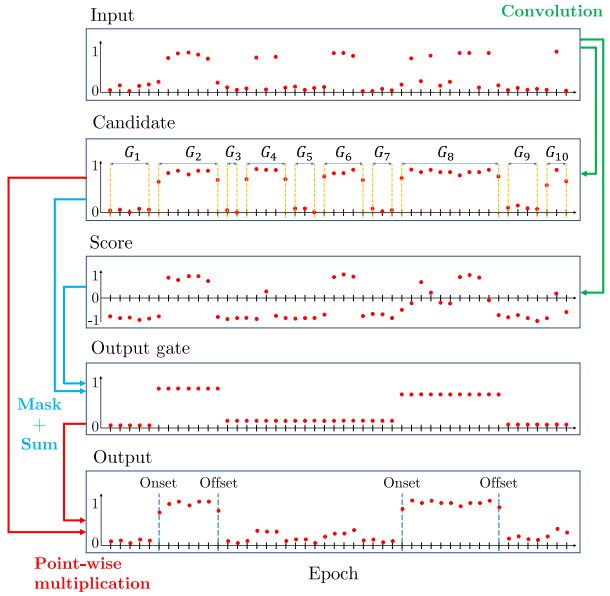

Fig. 3. Illustration of ScoreNet when $w = 1$. Only two groups, *i.e.*, G_2 and G_8, have adequate scores resulting in final predicted events.

incorporated into the procedure to improve seizure detection accuracy upon the first seizure classification step.

B. ScoreNet

ScoreNet is a proposed onset-offset detector that takes epochs with detected likelihood of seizure as an input (z) and returns a screened detection of seizures in terms of probabilities as the output ($\hat{y}$), as shown in Figure 2. A key to ScoreNet's success is to use a convolution to connect adjacent epoch-based classification results into consideration at the same time. Moreover, the concept of automatically selecting a cell to be an output is used to predict a seizure event. Figure 3 shows ScoreNet's computation process.

First, a *seizure candidate* c_i is defined as an epoch that has potentiality of containing a seizure by taking a convolution of neighbor epochs z_i with a linear filter a_1 of length $2w+1$ and passing through the sigmoid function to return a value ranging from zero to one.

$$c_i = \sigma\left(\mathbf{z}_i^T a_1 + b_1\right), \quad i = 1, 2, \ldots, N. \tag{1}$$

In the above, σ is a sigmoid function, $\mathbf{z}_i = (z_{i+w}, \ldots, z_i, \ldots, z_{i-w})$, and $z_j = 0$ for $j \leq 0$ and $j > N$. Thresholding c_i gives a binary sequence, where values of $c_i \geq \gamma$ are given a value of 1, and zero otherwise. The same consecutive values of the thresholded seizure candidate sequence are then clustered into groups, each denoted by G_l. We also assign a degree to which each epoch influences the positive predictions of its neighbor epochs through a score s_i, defined by

$$s_i = \tanh\left(\mathbf{z}_i^T a_2 + b_2\right), \quad i = 1, 2, \ldots, N, \tag{2}$$

where a_2 is a vector of length $2w + 1$ and b_2 is a bias term. Due to the hyperbolic tangent's range, and through optimal selection of (a_2, b_2), we intend for $s_i < 0$ when $\mathbf{z}_i$ and its neighboring epochs are zero and $s_i > 0$ otherwise; thus, the score values can help distinguish between normal and seizure epochs. Then, each group of seizure candidates identified earlier are fed through a defined *output gate*, which is a nonlinear function of the averaged scores within a group to indicate the probability that the whole group is a seizure event, as in the expression

$$o_l = \sigma\left(\frac{a_3}{N_l}\sum_{j\in G_l} s_j + b_3\right), \tag{3}$$

where N_l is the group size, l is the group index, a_3 and b_3 are scalar parameters.

Finally, ScoreNet produces an output $\hat{y}_i$ which is a probability of seizure occurrence during seizure candidate c_i, obtained by masking the seizure candidate with the output gate of group G_l to which $\hat{y}_i$ belongs, as defined by

$$\hat{y}_i = \sigma\left(a_4 c_i o_l + b_4\right), \quad \forall i \in G_l, \tag{4}$$

where a_4 and b_4 are scalar parameters. Note that the expressions of c_i and s_i resemble node equations in neural networks that take a linear combination of inputs and pass the combination through a nonlinear activation. The output gate equation (3) is also similar to an output gate in LSTM. For these reasons, the ScoreNet can be intuitively regarded as a neural network-based model.

As we have seen from the derivation of $\hat{y}_i$ in (1)-(4), ScoreNet takes into consideration known temporal characteristics of seizures into its prediction of sequence z (series of epochs with suspected seizure activities) by convoluting z with linear filters (a_1 and a_2) and by using the knowledge of pre-determined seizure groups. By choosing optimal parameters, (a_i, b_i) for $i = 1, \ldots, 4$, ScoreNet's unprecedented approach of gathering information from neighboring EEG epochs should help it rule out unrealistic prediction outcomes, such as abrupt seizure activity changes within short durations.

Lastly, we note that ScoreNet is a more general framework extended from the counting-based approach in [34]. The model parameters were not optimally chosen in [34], but instead set as $a_1 = a_2 = \mathbf{1}, a_3 = a_4 = 1, b_1 = -1, b_2 = -2$, and $b_4 = 0$, where $\mathbf{1}$ indicates the vector of ones with a compatible size, and only b_3 can be tuned. Because [34] used the Heaviside step function in (1), and with z_i being either zero (normal brain activity) or one (seizure), seizure candicate (c_i) was obtained by counting seizures from adjacent epochs using a fixed threshold of b_1. Similarly, [34]'s treatment of (2), where neighboring epochs were counted, made it so that the score (s_i) was set to one depending on whether the neighboring count exceeded a fixed threshold b_2. Therefore, ScoreNet is expected to be an improvement over the counting-based method since its parameters can be optimized and selected.

C. Log-Dice Loss

To estimate parameters in ScoreNet, we will formulate a minimization of a loss function $\mathcal{L}$ defined as the discrepancy between y – a binary sequence of annotated seizures (or target), and $\hat{y}$ – a corresponding sequence of seizure probability generated by ScoreNet:

$$\text{minimize} \quad \mathcal{L}\left(y, \hat{y}\right) \tag{5}$$

over the ScoreNet parameters (a_i, b_i) for $i = 1, \ldots, 4$.

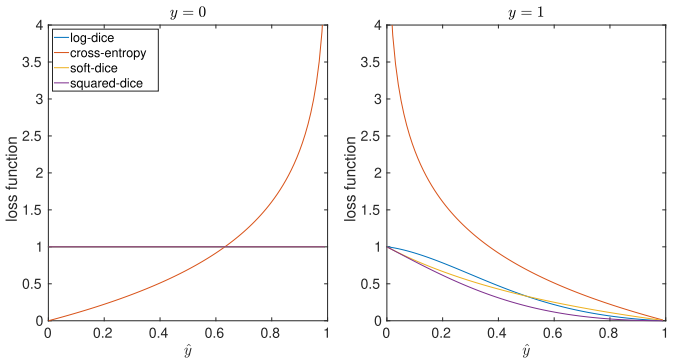

Fig. 4. Loss functions in binary classification and the proposed log-dice loss.

In a binary classification problem, many loss functions represent the similarity between $\hat{y}_i$ and y_i in different forms. It is important to note that EEG seizure detection is an imbalanced classification because most EEG epochs are normal (i.e., y_i's are 0). For example, a cross-entropy loss is commonly employed for training a classifier in many classification problems, but it is not suitable for imbalanced classification [36] since it penalizes losses in both data classes equally. Instead, imbalanced data problems are handled by data manipulation [37]–[40], or by introducing a loss function that penalizes each data class differently. Some examples of uneven penalization are the weighting entropy [41], or dice-coefficient-related loss [42], [43].

The dice similarity coefficient (DSC), or equivalently, the F_1 score is a measure of the similarity between a predicted outcome and the ground truth, defined by

$$\mathrm{DSC} = \frac{2\mathrm{TP}}{2\mathrm{TP} + \mathrm{FP} + \mathrm{FN}}, \tag{6}$$

where TP, FN, and FP are the numbers of true positives, false negatives, and false positives, respectively. Notice that the DSC does not take the true negative (TN) into account. This implies that when the DSC is used in model training, and when the negative refers to the normal class, the model parameters are optimized to favor improving the accuracy of detecting positives (in our case: seizure events) over the majority class (normal brain activity). Other variants of DSC also exist and are used in imbalanced classification, such as the soft-dice loss by [42] and the squared-dice loss[1] by [43].

In this work, we establish the *log-dice loss* variant of DSC to tackle our imbalanced data problem, defined as

$$\mathcal{L}_{\mathrm{logDL}}\left(y, \hat{y}\right) = 1 - \frac{2\sum_{i=1}^{N} y_i \log(1-\hat{y}_i)}{\sum_{i=1}^{N}\left[(1+y_i)\log(1-\hat{y}_i) + y_i \log \hat{y}_i\right]}. \tag{7}$$

The log-dice loss is equal to $1-\mathrm{DSC}$ when substituting TP, FN, and FP in (6) for $-\sum_i y_i \log(1-\hat{y}_i)$, $-\sum_i y_i \log \hat{y}_i$, and $-\sum_i (1-y_i)\log(1-\hat{y}_i)$, respectively.

The value of $\mathcal{L}_{\mathrm{logDL}}$ is in the range of $(0, 1]$ and decreases as y and $\hat{y}$ become more similar. $\mathcal{L}_{\mathrm{logDL}}$ reaches its maximum of one (worst score) under two cases: i) when $y = 0$ (all samples are normal), regardless of the prediction $\hat{y}$ because the index does not consider TN; or ii) when $y = 1$ and $\hat{y} = 0$ (no TP in the prediction). Figure 4 compares the cross-entropy, soft-dice, squared-dice and log-dice loss functions as $\hat{y}$ varies under two values of y (one-sample case for illustration). When $y = 0$, $\mathcal{L}_{\mathrm{logDL}}$'s constant loss means that the normal class is neglected when optimizing model parameters. On the other hand, when $y = 1$, and $\hat{y} \leq 0.5$, the log-dice loss has a higher penalty than the cross-entropy, soft-dice and squared-dice losses, implying that $\mathcal{L}_{\mathrm{logDL}}$ optimizes model parameters to prevent FN better than the other losses.

To solve (5), we apply a nonlinear conjugate gradient method because it has been shown to converge faster than other methods when training neural networks with limited variables (eight) to optimize [44].[2]

III. Effective Latency Index

We propose the *effective latency index (EL-index)* as an indicator of delays between detected and actual onset-offsets, while also taking undetected events into account. The EL-index gives a zero (worst) score to any undetected event, and a positive score to any correctly detected event where the score increases as the delay decreases. Suppose there are n actual seizure activities and k_i is an indicator of event i being detected, i.e., $k_i = 1$ when the event is correctly detected, and $k_i = 0$ otherwise. We also denote $d_i > 0$ and $d_i < 0$ for early and late detection of seizure onset and offset, respectively; note that d_i is not defined for an undetected seizure event. For a given $0 < r < 1$, the EL-index is defined as

$$\text{EL-index} = \frac{1}{n}\sum_{i=1}^{n} k_i r^{|d_i|}. \tag{8}$$

Index values can range from zero (missing all seizure events) to one (perfectly detecting all events). A large latency in the detection of any event will cause an exponential decrease in the EL-index at a decay rate of r. If we denote GDR (good detection rate) as a portion of correctly detected seizure events in one record given by $(1/n)\sum_{i=1}^{n} k_i$, then the EL-index can be regarded as an exponentially weighted GDR, and that it satisfies the bounds:

$$\mathrm{GDR} \cdot r^{|d|_{\max}} \leq \text{EL-index} \leq \mathrm{GDR}, \tag{9}$$

where $|d|_{\max}$ is the maximum value of absolute time delays. It is evident that the EL-index cannot be higher than GDR, while also being lower-bounded by the function $\mathrm{GDR} \cdot r^{|d|}$. Moreover, a relation between the EL-index and the mean absolute latency (MAL) can be derived and provides some connection about empirical distributions of collected time delays. Suppose we have time delay samples from two test results that have the same MAL and GDR; however, the first set contains narrowly distributed time delays, i.e., $d_i \approx \pm\mathrm{MAL}$, whereas the samples of the second set are highly varied. For the first set, the EL-index can be approximated by

$$\text{EL-index} \approx \mathrm{GDR} \cdot r^{\mathrm{MAL}}. \tag{10}$$

In contrast, when the time delays are widely spread, the approximation (10) does not hold, and the EL-index is always

[1]The actual function name in [43] is the *soft-dice loss*. We refer to it by a different name to avoid confusion.

[2]The authors thank Dr. Suchin Arunsawatwong for his advice about the algorithm.

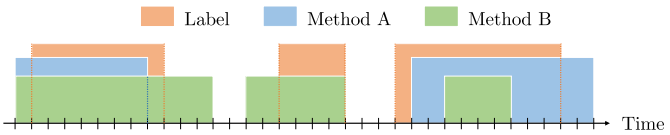

		Average latency	Average of absolute latency	EL-index
Onset	Method A	0.00	1.00	0.60
	Method B	0.00	2.00	0.81
Offset	Method A	0.50	1.50	0.57
	Method B	0.00	2.00	0.82

Fig. 5. Example of time-based measurements. Orange segments are annotated EEG epochs, whereas blue and green segments are predicted seizure epochs from methods A and B, respectively.

higher than that in the case of narrowly distributed latencies:

$$\mathrm{GDR}\cdot r^{\mathrm{MAL}} \le \mathrm{GDR}\cdot \frac{\sum_{i=1}^{n} k_i r^{|d_i|}}{\sum_{i=1}^{n} k_i} = \frac{1}{n}\sum_{i=1}^{n} k_i r^{|d_i|}. \quad (11)$$

We will use a hypothetical example illustrated in Figure 5 to demonstrate the EL-index's superiority in describing latency error in detected signals over using the mean latency as in [33], [35]. The values in Figure 5 show the comparison between the mean latency, MAL, and EL-index when $r = 0.9$. While methods A and B both have zero mean latencies of onset detection in this hypothetical example, neither perfectly detected seizure onsets; hence, this example shows that the mean latency can give a false sense of accuracy in the detection method. Next, if MAL is considered instead of the mean latency, method A still suggests higher detection accuracy (less latency and smaller MAL value) than method B, even though method A completely missed detecting the second seizure event ($k_2 = 0$). Once again, this example has shown that even MAL is not a good indicator of detector latency if there are many undetected events. However, the EL-index in this example does reveal that method B performs better than method A in detecting onsets, because the EL-index considers the fact that method A did not detect the second seizure event. Also, looking at Figure 5, it is apparent that method A detects onsets more accurately than offsets, which is correctly indicated by method A's higher EL-index of detecting onsets than offsets.

IV. Experiment

A. Data Preparation

We focus on using a patient-specific detection scheme to verify ScoreNet's performances when the heterogeneity in patients was controlled, and scalp EEG signals were used. For these reasons, the CHB-MIT Scalp EEG database [45], [46] publicly available on PhysioNet (https://physionet.org/content/chbmit/1.0.0/) and containing scalp signals is chosen. EEG signals in this database were observed from 24 pediatric cases of the age range 1.5-22 years at the Children's Hospital Boston, and the types of seizures vary across the patients; see more details in [8], [32]. The data were sampled at a rate of 256 Hz and a resolution of 16 bits; they were recorded with the international 10–20 electrode system. Most records consist of 23 channels collected from either referential or bipolar montages; for more details of the number of records, please see Table I. Since the data were recorded with both referential and bipolar montages, the EEG records were firstly rearranged to the bipolar montage system. The sequential order of the modified 18 channels were *FP1-F7, F7-T7, T7-P7, P7-O1, FP1-F3, F3-T3, T3-P3, P3-O1, FP2-F4, F4-C4, C4-P4, P4-O2, FP2-F8, F8-T8, T8-P8, P8-O2, FZ-CZ*, and *CZ-PZ*. The long EEG records were segmented into non-overlapping epochs of one second.

TABLE I
Summary of the CHB-MIT Scalp EEG Database

Cases	# records	Total duration (sec)	# seizures	Seizure duration (sec)
chb01	42	145,988	7	449
chb02	36	126,959	3	175
chb03	38	136,806	7	409
chb04	42	561,834	4	382
chb05	39	140,410	5	563
chb06	18	240,246	10	163
chb07	19	241,388	3	328
chb08	20	72,023	5	924
chb09	19	244,338	4	280
chb10	25	180,084	7	454
chb11	35	123,257	3	809
chb12	24	85,300	40	1,515
chb13	33	118,800	12	547
chb14	26	93,600	8	177
chb15	40	144,036	20	2,012
chb16	19	68,400	10	94
chb17	21	75,624	3	296
chb18	36	128,285	6	323
chb19	30	107,746	3	239
chb20	29	99,366	8	302
chb21	33	118,189	4	203
chb22	31	111,611	3	207
chb23	9	95,610	7	431
chb24	22	76,640	16	527
sum	**686**	**3,536,540**	**198**	**11,809**

In this work, no additional pre-processing methods such as artifact removal were performed because of the following reasons. To resemble most real applications, the EEG records were not perfectly clean for the detection to avoid too optimistic results. Besides, an artifact removal process, if done inappropriately, could deteriorate temporal and spatial patterns underlying seizure characteristics and further affect the detection performance. For these reasons, we decided to use the EEG data without removing artifacts for seizure detection.

B. Evaluation

Seizure detection methods were evaluated using a patient-specific leave-one-record-out cross validation (LOOCV) scheme, where *all records* in the CHB-MIT Scalp EEG database were used. Training and test data were taken from the same patient but different records. Detection methods were validated with all patient cases; they were assessed using event-based, epoch-based, and time-based metrics [5], [47]. The event-based metrics included good detection rate (GDR) and false positive rate per hour (FPR/h). The epoch-based metric was F_1, which fairly assesses seizure detection results as it is an imbalanced classification [48]. The time-based metric was the EL-index as explained in Section III. We also

used our detection results to compare the EL-index with other latency indices. If one true event was interpreted as more than one event by a detector, then the onset of the *first* predicted event and the offset of the *last* positive activity were used to calculate the time-based metrics.

C. Experimental Setup

The first-stage seizure detection in Figure 2 was performed by five classifiers: CNN, logistic regression, linear SVM, decision tree, and random forest. For CNN, we adopted the structure in [34] that can extract meaningful features from raw EEG segments which is the input as shown in Figure 6. Two 1D convolutional layers (Conv) are designed to effectively extract temporal and spatial features of the input. The first filter is to learn temporal characteristics of seizures, and the other filter can be interpreted as a feature extractor in the spatial domain; see more details of the design in [34]. The other classifiers depended on widely-used features that characterize ictal and normal patterns as reported in [3], [5], [8], [49]. *Time-domain features* computed from raw EEG epochs were the variance, energy, nonlinear energy, Shannon entropy, sample entropy, and approximate entropy. *Frequency-domain features* calculated from power spectral densities were the energies from eight sub-bands in the range of 0–25 Hz. In addition, *time-frequency-domain features* were extracted with discrete wavelet transform coefficients from five decomposition levels with the Daubechies 4 tap wavelet; these features were the mean absolute value, variance, energy, maximum, minimum, and line length. Features were extracted from each channel in an EEG epoch and normalized to a z-score. In total, 900 features were combined into a feature vector for the classification of EEG epochs.

As for the second-stage onset-offset detection of Figure 2, ScoreNet and the counting-based method were used and compared. The lengths of vectors a_1 and a_2 were set to 13 since these were the optimal parameter sizes of the counting-based method as reported in [34]. ScoreNet was trained with binary cross-entropy, soft-dice loss [42], and square-dice loss [43] for comparisons of dealing with an imbalanced data problem. Codes and results are available at https://github.com/Siyaosk129/ScoreNet.

V. Results and Discussions

Figures 7a and 7b show the GDR and FPR/h scores of every seizure-detection method we tested. Recall that our seizure-detection scheme was divided into two steps. The first-stage epoch-based classification was performed by CNN, logistic regression, linear SVM, decision tree, and random forest classifiers; GDR and FPR/h scores of performing only the first-stage classification with each of these classifiers are labeled as `classification`. The second step involved applying ScoreNet with different loss functions on the first-stage results; the loss functions used are labeled as in the parentheses as follows: entropy (`entropy`), soft-dice (`softdl`), squared-dice (`sqdl`), and log-dice (`logdl`). When the counting-based method was applied, we labeled

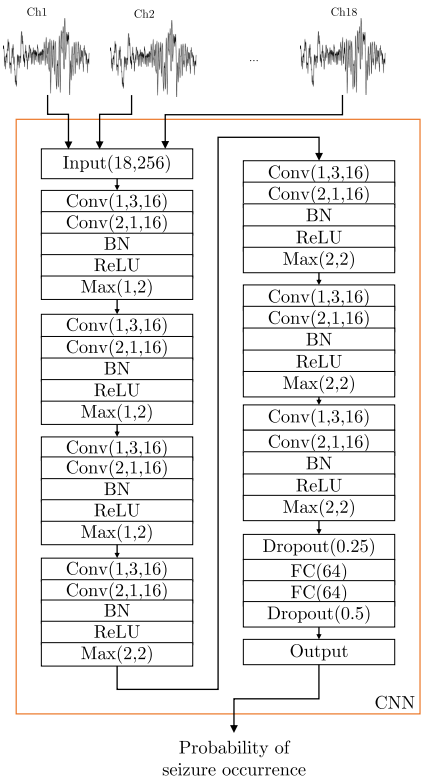

Fig. 6. CNN structure used in this work. Convolutional (Conv), batch normalization (BN), and max pooling (Max) layers are designed to effectively extract features from both temporal and spatial domains. ©2020 IEEE. Reproduced with permission.

these results as `counting`. We will describe and compare the results in three folds: the improvement of using onset-offset detection over epoch-based classification, a comparison between the counting-based and ScoreNet methods, and the accuracy of the onset-offset detection.

A. Seizure Detection

We can see the improved seizure detection results of applying ScoreNet over using only the classifiers in terms of F_1, GDR and FPR/h scores in Figures 7a and 7b and 8. Alone, the seizure classifiers detected seizure events at GDRs of more than 80%, but obtained F_1 of less than 40%, and had drastically varying FPR/h between 0.53 to 5.24 on average. If we consider all these scores as overall performance metrics, then random forest and CNN are both compromised classifiers that are good at detecting most seizure events, but at a cost of frequent erroneous inferences; both of these classifiers have room for improvement.

By applying ScoreNet with any of the loss functions, regardless of the classification methods, F_1 increased at least 18% over lone classifier F_1 scores, and FPR/h significantly reduced at least 0.36 times per hour; however, GDRs did drop slightly, except in the case of random forest where the GDR increased up to 7%. The favorable outcomes afforded by combining random forest and ScoreNet are exemplified by the example case illustrated in Figure 9. Random forest produced an interval of small seizure probabilities that were sufficiently distinguishable from the background for ScoreNet to recognize them as seizure events and significantly boost the

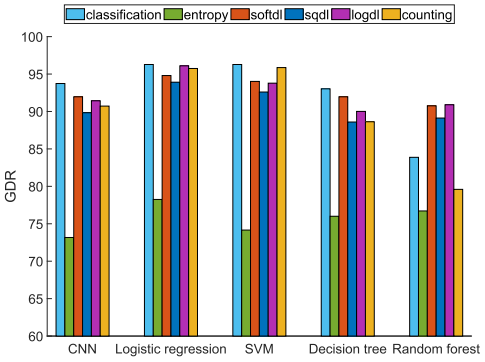

(a) GDR.

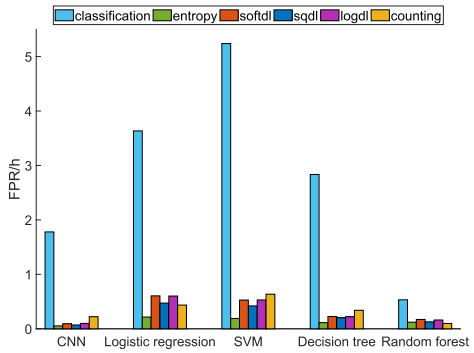

(b) FPR/h.

Fig. 7. Comparisons of averaged GDR and FPR/h from test cases using different epoch-based seizure detection methods.

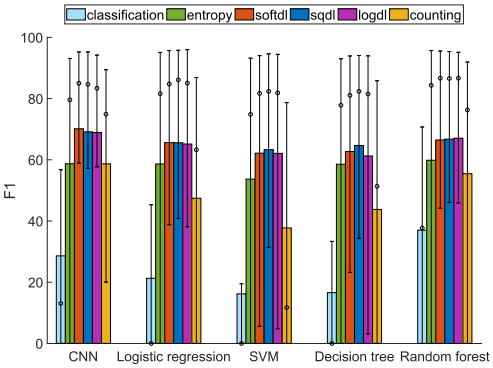

Fig. 8. Comparisons of F_1 obtained from test cases using different epoch-based seizure detection methods. Color bars indicate the average values of all test records; circle markers present the median; vertical bars show the interquartiles.

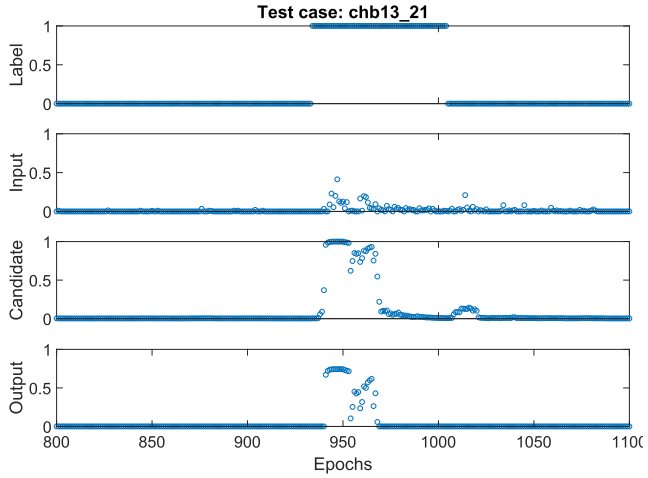

Fig. 9. Example of ScoreNet result (test case `chb13_21`) when the log-dice loss and random forest are used.

magnitudes of their candidate and output scores. Thus, this confirmed that using ScoreNet, with any dice loss function, generally improves epoch-based classification performances; specifically, ScoreNet can indicate some seizure events that are not detected by a lone classification process. Secondly, this also confirmed that dice loss functions are appropriate for handling imbalanced-class data problems.

Since the application of ScoreNet resulted in FPR/h and F_1 score improvements but GDR drop-offs, we can generally interpret that FP, FN, and TP decreased with ScoreNet present, and the extent to which these predictions were eliminated depended on the employed cost function. For example, using ScoreNet with the cross-entropy loss, which mainly penalizes errors of normal/majority class samples, resulted in a large reduction of FPR/h. This was the result of ScoreNet with cross-entropy reducing several isolated FPs at the expense of also unfavorably removing some TPs, where perhaps the seizures only occurred within a few epochs that did not generate enough predicted positives for event detection.

For dice loss functions, ScoreNet generally yields similar seizure detection performances across any seizure detection methods. ScoreNet with the soft-dice loss provided the best general seizure-activity detection results, although ScoreNet with the squared-dice loss provided better (lower) FPR/h. In addition, using the log-dice loss improved classification performance when classification errors were large. Referring again to the results of using random forest and log-dice loss in Figure 9, random forest was initially unable to detect the seizure in epochs 940–1000, where the seizure probability inputs were smaller than 0.5. However, by incorporating ScoreNet, the seizure predictions in epochs 940–1000 were boosted enough that these epochs ended up having active seizure labels as well. Thus, it was the log-dice loss's ability to uncover previously undetected seizure activities that resulted in better GDR and F_1 scores, and made it the form of dice-loss that most improved the random forest classifier.

Table II summarizes previous studies' seizure detection performances, with the amount of data and validation schemes they used. In our study, the highest F_1 score was achieved by ScoreNet with soft-dice loss and CNN as the prior classifier; therefore, we compared the performance of this method (`proposed method`) to the previous references. It was difficult to directly compare the performance metrics since the validation schemes and data selection were different among these studies. Many of the previous studies selected specific records from the database, and only a few applied LOOCV as a validation scheme. [52] used only records containing seizures in the experiment, and [50], [54] did not report on their data specification nor validation scheme. Moreover, some studies performed data sampling to create balanced training data [6], but in practice some EEG characteristics – such as rarity and types – cannot be accurately selected; it is more clinically challenging to use all data and apply LOOCV to

TABLE II
COMPARISON OF SEIZURE DETECTION METHODS USING CHB-MIT DATABASE

Reference	Detection type	Data specification	Validation	Method	Acc	Sen	Spec	F_1	GDR	FPR/h
[7]	Event	Long seizures	No CV	aEEG + adaptive threshold	NR	NR	NR	NR	88.50	0.18
[50]†	Event	NR	NR	Spectrogram + mSSDA	93.82	NR	NR	96.05	NR	NR
[20]	Event	Specific records (22 cases)	LOOCV	Energy and fractal	NR	NR	NR	NR	97.00	0.10
[51]†	Event	166 mins (11 cases) 70% training data	No CV	PSD + CNN-based ensemble	92.60	92.30	97.00	NR	NR	NR
[28]	Event	All, Balanced training data	No CV	Statistical features + Bi-LSTM	92.66	93.61	91.85	NR	NR	NR
[8]*	Onset	NR	LOOCV	Energy + RBF SVM	NR	NR	NR	NR	96.00	0.08
[52]	Onset	Seizure in record	LOOCV	Unified multi-level spectral-temporal feature + RBF SVM	97.80	NR	NR	78.00	97.20	0.64
[53]	Onset	Seizures in record (21 cases)	LOOCV	Channel-embedding temporal-spectral squeeze-and-excitation network	95.96	92.41	96.05	NR	98.93	NR
[54]	Onset	31.6 hrs training data, 945.3 hrs test data	NR	DWT + EMD + common spatial pattern + SVM-based ensemble	97.49	97.34	97.50	NR	98.74	0.63
[33]†	Onset/offset	Bipolar montage (18 cases), Balanced training data	10-fold	Relative band energy + LDA	NR	NR	99.99	NR	92.60	0.30
[35]	Onset/offset	397 hrs (18 cases), 60% training data	5-fold	Statistical features + LDA	98.00	NR	98.05	NR	100.00	4.02
[34]	Onset/offset	All	LOOCV	CNN + counting-based method	99.72	72.78	99.82	64.40	83.41	0.12
Proposed method	Onset/offset	All	LOOCV	CNN + ScoreNet (soft-dice loss)	99.83	76.54	99.92	70.15	91.96	0.09

NR = no report, All = use full data set, † Apply patient non-specific scheme or no report, * Use median instead of mean in the report.

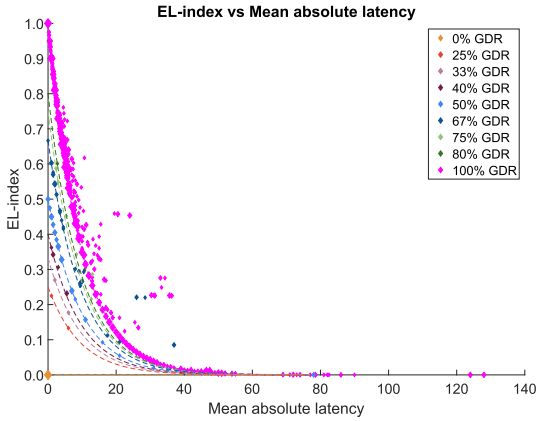

Fig. 10. Relation of EL-index and mean absolute latency (MAL) from the test data given $r = 0.9$. Marker sizes are proportional to the number of samples in a log scale. Dashed line illustrates GDR $\cdot\, r^{|d|}$ limits.

verify the detection performance. With these considerations in mind, our proposed method yielded competitive performances against previous results.

B. Onset and Offset Determination

The GDR, MAL, and corresponding EL-indices of every test results are displayed in Figure 10. Although delay is not defined when the GDR = 0%, we have set d to zero (indicated by yellow markers) in these cases for illustrative purposes. There were a significant number of test cases with 0% GDR, or undetected events. Hence, using only the MAL as a performance metric would mistakenly ignore these detection failures, whereas the EL-index captures undetected events since 0% GDR is still reflected by a zero EL-index score. For low GDR cases (about 40–50%), seizure events appeared to be randomly detected, which still resulted in misleadingly low MAL scores in some test samples, but were properly reflected by the decreased EL-index scores (indicating worse performance). These observations suggest that the proposed EL-index is more suitable as a time-based index than the MAL.

For any non-zero GDR case, the EL-index was biased to have higher values when many seizure events are detected, and the latencies in those detected seizure onset/offsets are

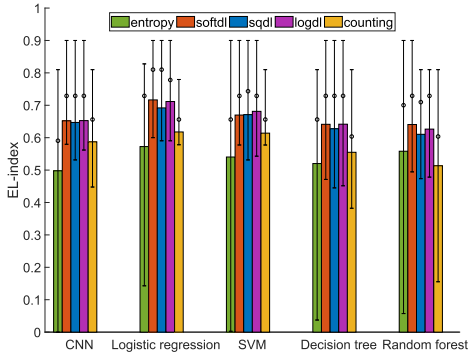

(a) Seizure onset.

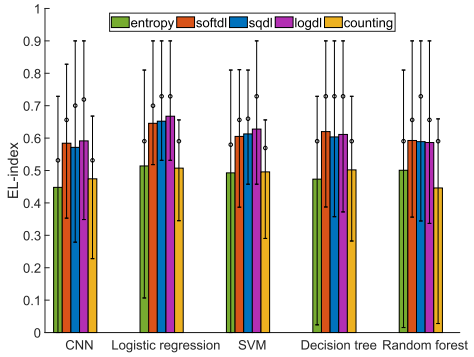

(b) Seizure offset.

Fig. 11. Onset-offset detection performances measured by EL-index. The color bars indicate averaged values; circle markers present the median; vertical bars show the interquartiles.

insignificant. In Figure 10, the relationship between EL-index and MAL mostly satisfies the exponential bound (9), GDR$\cdot r^{|d|}$ represented by dashed lines. As analyzed in Section III, this means that latencies in detected seizure onset/offsets generally had low variation. In addition, the MAL cannot provide information on whether different cases with similar MAL scores have similar or different onset-offset latencies, but the EL-index values can. Therefore, the EL-index provides not only insight into the accuracy of seizure onset-offset detection, but also the accuracy of seizure event detection, and interpretation of the empirical distributions of latencies when considered jointly with the GDR.

TABLE III
THE AVERAGE EL-INDEX OF SEIZURE ONSET AND OFFSET DETERMINATION. FOR EACH CLASSIFIER, THE BOLDFACE VALUE IS THE MAXIMUM EL-INDEX

		CNN	Logistic regression	SVM	Decision tree	Random forest
Onset	entropy	0.50	0.57	0.54	0.52	0.56
	softdl	**0.65**	**0.72**	0.67	**0.64**	**0.64**
	sqdl	**0.65**	0.69	0.67	0.63	0.61
	logdl	**0.65**	0.71	**0.68**	**0.64**	0.63
	counting	0.59	0.62	0.61	0.55	0.51
Offset	entropy	0.45	0.51	0.49	0.47	0.50
	softdl	0.58	0.65	0.61	**0.62**	**0.59**
	sqdl	0.57	0.65	0.61	0.60	**0.59**
	logdl	**0.59**	**0.67**	**0.63**	0.61	**0.59**
	counting	0.47	0.51	0.50	0.50	0.45

Figure 11 compares the performances of detecting onsets versus offsets as measured by the EL-index with $r = 0.9$. In the case of seizure onset detection, the mean EL-indices were in the range of 0.50–0.71 and the medians ranged from 0.59 to 0.81. As for detecting seizure offset, the mean and median ranges of EL-indices were slightly lower 0.45–0.67 and 0.53–0.73, respectively. As the minimum median (among several classifiers) was around 0.53, we can interpret together with Figure 10 that around half of the test samples were detected seizures with a MAL of less than 10 seconds, which is clinically acceptable.

Table III compiles the EL-indices obtained from the detection methods with various choices of loss functions and classifiers. The EL-indices obtained by using the dice loss functions were similarly high compared to those of the entropy loss and the counting-based method; in particular, the log-dice loss achieved slightly better EL-indices than other dice loss functions. Also, all methods indicated the seizure onsets better than the seizure offsets. This is due to the characteristics of epileptic seizures where ictal patterns occurring at the event ending are typically less dominant than the patterns at the beginning, and so it is harder for detectors to distinguish seizure epochs near the end of events. Recall that the log-dice loss can fix classification outcomes that are erroneously labeled as negatives due to low seizure probabilities; we now also know that these errors tend to occur at the end of seizure event, and we should see the most performance improvements when employing the log-dice loss in cases where large numbers of these classification errors occur.

VI. CONCLUSION

This research established an automatic epileptic seizure onset and offset detection scheme composed of two processes: detecting seizures in epochs from EEG signals, and determining the beginning and ending points of a seizure event. ScoreNet was designed to detect epileptic seizure onsets and offsets from the first-stage epoch-based classification results. It incorporates a log-dice loss function to handle the data class imbalance that is inherent in using EEG signals to classify seizure events. Its ability to detect seizure onset/offsets was demonstrated by a proposed EL-index. The proposed scheme was evaluated with real patient cases from the CHB-MIT Scalp EEG database. In handling these cases, ScoreNet performed better than a lone epoch-based seizure classification method with improved F_1 scores of up to 70.15%, dramatically reduced the false alarms rates to 0.05 times per hour, and yielded onset-offset detection errors of typically less than 10 seconds, which are clinically acceptable. Performance improvements yielded using the log-dice loss were most pronounced when prediction errors from epoch-based seizure detection were large. In addition, the EL-index was proven to be suitable for measuring seizure onset/offset detection latencies, as it provides information about both the correct detection of seizure events, and the latency distribution.

VII. LIMITATIONS AND FUTURE WORK

While our method provides several advantages over previous seizure detection methods, some limitations and concerns with it are worth noting. First, we employed a patient-specific scheme in this paper to prove ScoreNet's ability to improve seizure detection performance. As such, the diversity of seizure types and artifact degrees in different patients may have been left out of consideration if ScoreNet's enhancement ability is unique to each patient. Since ScoreNet has to be specifically trained for each patient, EEG recordings and seizure annotations must first be collected from a patient to initially train the model. This limits the models practicality, raising the concept of a universally pre-trained detector. Perhaps ScoreNet can be trained across patients or on a larger dataset, but how the average detection performance would respond is yet to be seen, especially considering the high EEG variations between patients. In addition, we have validated an ensemble model of patient-specific CNN models on other patients' records. The epoch-based seizure predictions were always negative, and F_1 scores were all zero for every test case. Moreover, seizure probabilities of abnormal epochs were not sufficiently large for ScoreNet to differentiate seizures from EEG background signals. This suggests that an extension on detection universality should be considered in the future. Hence, future work could focus on developing a universal seizure detector that exploits common seizure characteristics across various patients.

REFERENCES

[1] R. S. Fisher *et al.*, "ILAE official report: A practical clinical definition of epilepsy," *Epilepsia*, vol. 55, no. 4, pp. 475–482, 2014.
[2] D. J. Thurman *et al.*, "Standards for epidemiologic studies and surveillance of epilepsy," *Epilepsia*, vol. 52, pp. 2–26, Sep. 2011.
[3] U. R. Acharya, H. Fujita, V. K. Sudarshan, S. Bhat, and J. E. Koh, "Application of entropies for automated diagnosis of epilepsy using EEG signals: A review," *Knowl. Based Syst.*, vol. 88, pp. 85–96, Nov. 2015.
[4] T. Alotaiby, F. E. A. El-Samie, S. A. Alshebeili, and I. Ahmad, "A review of channel selection algorithms for EEG signal processing," *EURASIP J. Adv. Signal Process.*, vol. 2015, no. 1, pp. 66–86, Dec. 2015.
[5] P. Boonyakitanont, A. Lek-uthai, K. Chomtho, and J. Songsiri, "A review of feature extraction and performance evaluation in epileptic seizure detection using EEG," *Biomed. Signal Process. Control*, vol. 57, Mar. 2020, Art. no. 101702.
[6] A. R. Hassan, A. Subasi, and Y. Zhang, "Epilepsy seizure detection using complete ensemble empirical mode decomposition with adaptive noise," *Knowl.-Based Syst.*, vol. 191, Mar. 2020, Art. no. 105333.
[7] C. Satirasethawong, A. Lek-Uthai, and K. Chomtho, "Amplitude-integrated EEG processing and its performance for automatic seizure detection," in *Proc. IEEE Int. Conf. Signal Image Process. Appl. (ICSIPA)*, Oct. 2015, pp. 551–556.
[8] A. Shoeb and J. Guttag, "Application of machine learning to epileptic seizure detection," in *Proc. 27th Int. Conf. Mach. Learn.*, 2010, pp. 975–982.

[9] S. Altunay, Z. Telatar, and O. Erogul, "Epileptic EEG detection using the linear prediction error energy," *Expert Syst. Appl.*, vol. 37, no. 8, pp. 5661–5665, 2010.

[10] K. Samiee, P. Kovács, and M. Gabbouj, "Epileptic seizure classification of EEG time-series using rational discrete short-time Fourier transform," *IEEE Trans. Biomed. Eng.*, vol. 62, no. 2, pp. 541–552, Feb. 2015.

[11] M. Li, W. Chen, and T. Zhang, "Classification of epilepsy EEG signals using DWT-based envelope analysis and neural network ensemble," *Biomed. Signal Process. Control*, vol. 31, pp. 357–365, Jan. 2017.

[12] N. S. Tawfik, S. M. Youssef, and M. Kholief, "A hybrid automated detection of epileptic seizures in EEG records," *Comput. Elect. Eng.*, vol. 53, pp. 177–190, Jul. 2016.

[13] P. Li, C. Karmakar, J. Yearwood, S. Venkatesh, M. Palaniswami, and C. Liu, "Detection of epileptic seizure based on entropy analysis of short-term EEG," *PLoS ONE*, vol. 13, no. 3, Mar. 2018, Art. no. e0193691.

[14] V. Gupta and R. B. Pachori, "Epileptic seizure identification using entropy of FBSE based EEG rhythms," *Biomed. Signal Process. Control*, vol. 53, Aug. 2019, Art. no. 101569.

[15] T. S. Kumar, V. Kanhangad, and R. B. Pachori, "Classification of seizure and seizure-free EEG signals using local binary patterns," *Biomed. Signal Process. Control*, vol. 15, pp. 33–40, Jan. 2015.

[16] A. K. Jaiswal and H. Banka, "Local pattern transformation based feature extraction techniques for classification of epileptic EEG signals," *Biomed. Signal Process. Control*, vol. 34, pp. 81–92, Apr. 2017.

[17] Y. Li, W.-G. Cui, H. Huang, Y.-Z. Guo, K. Li, and T. Tan, "Epileptic seizure detection in EEG signals using sparse multiscale radial basis function networks and the Fisher vector approach," *Knowl.-Based Syst.*, vol. 164, pp. 96–106, Jan. 2019.

[18] M. Mursalin, Y. Zhang, Y. Chen, and N. V. Chawla, "Automated epileptic seizure detection using improved correlation-based feature selection with random forest classifier," *Neurocomputing*, vol. 241, pp. 204–214, Jun. 2017.

[19] E. Alickovic, J. Kevric, and A. Subasi, "Performance evaluation of empirical mode decomposition, discrete wavelet transform, and wavelet packed decomposition for automated epileptic seizure detection and prediction," *Biomed. Signal Process. Control*, vol. 39, pp. 94–102, Jan. 2018.

[20] L. S. Vidyaratne and K. M. Iftekharuddin, "Real-time epileptic seizure detection using EEG," *IEEE Trans. Neural Syst. Rehabil. Eng.*, vol. 25, no. 11, pp. 2146–2156, Nov. 2017.

[21] P. Fergus, A. Hussain, D. Hignett, D. Al-Jumeily, K. Abdel-Aziz, and H. Hamdan, "A machine learning system for automated whole-brain seizure detection," *Appl. Comput. Informat.*, vol. 12, pp. 70–89, Jan. 2016.

[22] R. San-Segundo, M. Gil-Martín, L. F. D'Haro-Enríquez, and J. M. Pardo, "Classification of epileptic EEG recordings using signal transforms and convolutional neural networks," *Comput. Biol. Med.*, vol. 109, pp. 148–158, Jun. 2019.

[23] A. Shoeibi *et al.*, "Epileptic seizures detection using deep learning techniques: A review," 2020, *arXiv:2007.01276*.

[24] H. Takahashi, A. Emami, T. Shinozaki, N. Kunii, T. Matsuo, and K. Kawai, "Convolutional neural network with autoencoder-assisted multiclass labelling for seizure detection based on scalp electroencephalography," *Comput. Biol. Med.*, vol. 125, Jun. 2020, Art. no. 104016.

[25] A. Shoeibi *et al.*, "A comprehensive comparison of handcrafted features and convolutional autoencoders for epileptic seizures detection in EEG signals," *Expert Syst. Appl.*, vol. 163, Jan. 2021, Art. no. 113788.

[26] U. R. Acharya, S. L. Oh, Y. Hagiwara, J. H. Tan, and H. Adeli, "Deep convolutional neural network for the automated detection and diagnosis of seizure using EEG signals," *Comput. Biol. Med.*, vol. 100, pp. 270–278, Sep. 2017.

[27] X. Tian *et al.*, "Deep multi-view feature learning for EEG-based epileptic seizure detection," *IEEE Trans. Neural Syst. Rehabil. Eng.*, vol. 27, no. 10, pp. 1962–1972, Oct. 2019.

[28] X. Hu, S. Yuan, F. Xu, Y. Leng, K. Yuan, and Q. Yuan, "Scalp EEG classification using deep bi-LSTM network for seizure detection," *Comput. Biol. Med.*, vol. 124, Sep. 2020, Art. no. 103919.

[29] A. O'Shea, G. Lightbody, G. Boylan, and A. Temko, "Neonatal seizure detection from raw multi-channel EEG using a fully convolutional architecture," *Neural Netw.*, vol. 123, pp. 12–25, Mar. 2020.

[30] A. Emami, N. Kunii, T. Matsuo, T. Shinozaki, K. Kawai, and H. Takahashi, "Seizure detection by convolutional neural network-based analysis of scalp electroencephalography plot images," *NeuroImage, Clin.*, vol. 22, Jan. 2019, Art. no. 101684.

[31] I. Covert *et al.*, "Temporal graph convolutional networks for automatic seizure detection," 2019, *arXiv:1905.01375*.

[32] A. Shoeb, A. Kharbouch, J. Soegaard, S. Schachter, and J. Guttag, "An algorithm for detecting seizure termination in scalp EEG," in *Proc. Annu. Int. Conf. Eng. Med. Biol. SoC.*, 2011, pp. 1443–1446.

[33] L. Orosco, A. G. Correa, P. Diez, and E. Laciar, "Patient non-specific algorithm for seizures detection in scalp EEG," *Comput. Biol. Med.*, vol. 71, pp. 128–134, Apr. 2016.

[34] P. Boonyakitanont, A. Lek-uthai, and J. Songsiri, "Automatic epileptic seizure onset-offset detection based on CNN in scalp EEG," in *Proc. Int. Conf. Acoust., Speech, Signal Process. (ICASSP)*, May 2020, pp. 1225–1229.

[35] G. Chandel, P. Upadhyaya, O. Farooq, and Y. U. Khan, "Detection of seizure event and its onset/offset using orthonormal triadic wavelet based features," *IRBM*, vol. 40, no. 2, pp. 103–112, Mar. 2019.

[36] T.-Y. Lin, P. Goyal, R. Girshick, K. He, and P. Dollar, "Focal loss for dense object detection," in *Proc. IEEE Int. Conf. Comput. Vis. (ICCV)*, Oct. 2017, pp. 2980–2988.

[37] I. Nekooeimehr and S. K. Lai-Yuen, "Adaptive semi-unsupervised weighted oversampling (A-SUWO) for imbalanced datasets," *Expert Syst. Appl.*, vol. 46, pp. 405–416, May 2016.

[38] J. Ha and J. Lee, "A new under-sampling method using genetic algorithm for imbalanced data classification," in *Proc. 10th Int. Conf. Ubiquitous Inf. Manage. Commun.*, 2016, pp. 1–6.

[39] C. Jian, J. Gao, and Y. Ao, "A new sampling method for classifying imbalanced data based on support vector machine ensemble," *Neurocomputing*, vol. 193, pp. 115–122, Jun. 2016.

[40] G. Haixiang *et al.*, "Learning from class-imbalanced data: Review of methods and applications," *Expert Syst. Appl.*, vol. 73, pp. 220–239, May 2017.

[41] B. Krawczyk, M. Woźniak, and G. Schaefer, "Cost-sensitive decision tree ensembles for effective imbalanced classification," *Appl. Soft Comput.*, vol. 14, pp. 554–562, Jan. 2014.

[42] R. Lguensat, M. Sun, R. Fablet, P. Tandeo, E. Mason, and G. Chen, "EddyNet: A deep neural network for pixel-wise classification of oceanic eddies," in *Proc. IGARSS - IEEE Int. Geosci. Remote Sens. Symp.*, Jul. 2018, pp. 1764–1767.

[43] F. Milletari, N. Navab, and S.-A. Ahmadi, "V-net: Fully convolutional neural networks for volumetric medical image segmentation," in *Proc. 4th Int. Conf. 3D Vis. (3DV)*, Oct. 2016, pp. 565–571.

[44] Q. V. Le, J. Ngiam, A. Coates, A. Lahiri, B. Prochnow, and A. Y. Ng, "On optimization methods for deep learning," in *Proc. 28th Int. Conf. Int. Conf. Mach. Learn.*, 2011, pp. 265–272.

[45] A. L. Goldberger *et al.*, "PhysioBank, PhysioToolkit, and PhysioNet," *Circulation*, vol. 101, no. 23, Jun. 2000.

[46] A. Shoeb, "Application of machine learning to epileptic seizure onset detection and treatment," Ph.D. dissertation, Harvard-MIT Division Health Sci. Technol., Massachusetts Inst. Technol., Cambridge, MA, USA, 2009.

[47] A. Temko, E. Thomas, W. Marnane, G. Lightbody, and G. B. Boylan, "Performance assessment for EEG-based neonatal seizure detectors," *Clin. Neurophysiol.*, vol. 122, no. 3, pp. 474–482, Mar. 2011.

[48] D. M. Powers, "Evaluation: From precision, recall and F-measure to ROC, informedness, markedness and correlation," *J. Mach. Learn. Technol.*, vol. 2, no. 1, pp. 37–63, 2011.

[49] U. R. Acharya, S. V. Sree, G. Swapna, R. J. Martis, and J. S. Suri, "Automated EEG analysis of epilepsy: A review," *Knowl.-Based Syst.*, vol. 45, pp. 147–165, Jun. 2013.

[50] Y. Yuan, G. Xun, K. Jia, and A. Zhang, "A multi-view deep learning method for epileptic seizure detection using short-time Fourier transform," in *Proc. 8th ACM Int. Conf. Bioinf., Comput. Biol., Health Informat.*, Aug. 2017, pp. 213–222.

[51] Y. Gao, B. Gao, Q. Chen, J. Liu, and Y. Zhang, "Deep convolutional neural network-based epileptic electroencephalogram (EEG) signal classification," *Frontiers Neurol.*, vol. 11, p. 375, May 2020.

[52] F.-G. Tang, Y. Liu, Y. Li, and Z.-W. Peng, "A unified multi-level spectral–temporal feature learning framework for patient-specific seizure onset detection in EEG signals," *Knowl.-Based Syst.*, vol. 205, Oct. 2020, Art. no. 106152.

[53] Y. Li, Y. Liu, W.-G. Cui, Y.-Z. Guo, H. Huang, and Z.-Y. Hu, "Epileptic seizure detection in EEG signals using a unified temporal-spectral Squeeze-and-Excitation network," *IEEE Trans. Neural Syst. Rehabil. Eng.*, vol. 28, no. 4, pp. 782–794, Apr. 2020.

[54] C. Li *et al.*, "Seizure onset detection using empirical mode decomposition and common spatial pattern," *IEEE Trans. Neural Syst. Rehabil. Eng.*, vol. 29, pp. 458–467, 2021.